JOURNAL OF BACTERIOLOGY, Mar. 2001, p. 1909–1920 Vol. 183, No. 6
0021-9193/01/$04.00+0 DOI: 10.1128/JB.183.6.1909–1920.2001

Analysis of the *pmsCEAB* Gene Cluster Involved in Biosynthesis of Salicylic Acid and the Siderophore Pseudomonine in the Biocontrol Strain *Pseudomonas fluorescens* WCS374

JESÚS MERCADO-BLANCO,[1]† KOEN M. G. M. VAN DER DRIFT,[2]‡ PER E. OLSSON,[1]
JANE E. THOMAS-OATES,[2]§ LEENDERT C. VAN LOON,[1]
AND PETER A. H. M. BAKKER[1]*

Department of Plant Ecology and Evolutionary Biology, Section of Plant Pathology, Utrecht University, 3508 TB Utrecht,[1] and Department of Mass Spectrometry, Utrecht University, 3584 CA Utrecht,[2] The Netherlands

Received 6 July 2000/Accepted 11 December 2000

Mutants of *Pseudomonas fluorescens* WCS374 defective in biosynthesis of the fluorescent siderophore pseudobactin still display siderophore activity, indicating the production of a second siderophore. A recombinant cosmid clone (pMB374-07) of a WCS374 gene library harboring loci necessary for the biosynthesis of salicylic acid (SA) and this second siderophore pseudomonine was isolated. The salicylate biosynthesis region of WCS374 was localized in a 5-kb *Eco*RI fragment of pMB374-07. The SA and pseudomonine biosynthesis region was identified by transfer of cosmid pMB374-07 to a pseudobactin-deficient strain of *P. putida*. Sequence analysis of the 5-kb subclone revealed the presence of four open reading frames (ORFs). Products of two ORFs (*pmsC* and *pmsB*) showed homologies with chorismate-utilizing enzymes; a third ORF (*pmsE*) encoded a protein with strong similarity with enzymes involved in the biosynthesis of siderophores in other bacterial species. The region also contained a putative histidine decarboxylase gene (*pmsA*). A putative promoter region and two predicted iron boxes were localized upstream of *pmsC*. We determined by reverse transcriptase-mediated PCR that the *pmsCEAB* genes are cotranscribed and that expression is iron regulated. In vivo expression of SA genes was achieved in *P. putida* and *Escherichia coli* cells. In *E. coli*, deletions affecting the first ORF (*pmsC*) diminished SA production, whereas deletion of *pmsB* abolished it completely. The *pmsB* gene induced low levels of SA production in *E. coli* when expressed under control of the *lacZ* promoter. Several lines of evidence indicate that SA and pseudomonine biosynthesis are related. Moreover, we isolated a Tn*5* mutant (374-05) that is simultaneously impaired in SA and pseudomonine production.

Despite its abundance in Earth's crust, iron is largely unavailable for microbial assimilation. Soil microorganisms have developed a mechanism that ensures iron availability in an environment that provides iron (Fe^{3+}) at only about 10^{-18} M. This strategy involves the secretion of low-molecular-weight iron-chelating compounds called siderophores (45) that show a considerable structural diversity and can be classified according to their main chelating groups (26). Bacteria produce a large variety of siderophores under iron-limiting conditions: hydroxamates, phenol-catecholates, and carboxylates. Moreover, some bacteria produce several types of siderophores, as described for strains of *Enterobacter cloacae* (37) and *Pseudomonas* spp. (2, 11, 43, 61, 64). Siderophores produced by certain strains of fluorescent *Pseudomonas* spp. have been linked to suppression of soil-borne plant diseases. It has been suggested that siderophores are antagonistic by means of sequestering iron from the environment, restricting growth of the pathogen (5, 34, 36). *Pseudomonas* siderophores have also been implicated in inducing systemic resistance (ISR) in plants (33, 40), that is, an enhancement of the defense capacity of the plant against a broad spectrum of pathogens, triggered by nonpathogenic plant growth-promoting rhizobacteria (63).

Another compound with siderophore activity that can be produced by microorganisms is salicylic acid (SA; 2-hydroxybenzoic acid), SA acting as an authentic, endogenous siderophore has been found under iron limitation in *Mycobacterium* spp. (51), *Pseudomonas* spp. (2, 3, 43, 64), *Azospirillum lipoferum* (54), and *Burkholderia (Pseudomonas) cepacia* (61). SA is also the precursor or intermediate in the biosynthesis of microbial siderophores, such as pyochelin in *Pseudomonas aeruginosa* (14). Mutants defective in SA production are unable to synthesize pyochelin (2). The salicylamide moiety is encountered not only in pyochelin but also in aeruginoic acid and pseudomonine produced by *P. fluorescens* strains (3, 12). SA has also been reported to be incorporated into mycobactin S produced by *Mycobacterium smegmatis* (27, 50), mycobactin T, isolated from *M. tuberculosis* (60), parabactin produced by *Paracoccus denitrificans* (47), and maduraferrin isolated from *Acinomadura madurae* (31). Finally, vulnibactin, a polyamine-containing siderophore from *Vibrio vulnificus*, contains two SA residues in its molecule (46).

* Corresponding author. Mailing address: Department of Plant Ecology and Evolutionary Biology, Section of Plant Pathology, Utrecht University, P.O. Box 800.84, 3508 TB Utrecht, The Netherlands. Phone: 31-30-2536861. Fax: 31-30-2518366. E-mail: P.A.H.M.Bakker@bio.uu.nl.

† Present address: Departamento de Protección de Cultivos, Instituto de Agricultura Sostenible (CSIC), 14080 Córdoba, Spain.

‡ Present address: Mass Spectrometry Resource, Department of Chemistry, Washington University, St. Louis, MO 63130.

§ Present address: Michael Barber Centre for Mass Spectrometry, Department of Chemistry, UMIST, Manchester M60 1QD, United Kingdom.

TABLE 1. Strains and plasmids used

Strain or plasmid	Characteristics	Reference or source
Strains		
P. fluorescens		
WCS374	Wild-type PGPR; Psb$^+$ Pms$^+$ SA$^+$	22
374-05	WCS374 Tn5 mutant; Psb$^+$ Pms$^-$ SA$^-$	This work
374-05.1	374-05 Tn5 (Tc^r) Psb$^-$ mutant derivative	This work
374-08	WCS374 Tn5 mutant; Psb$^-$ Pms$^+$ SA$^+$	This work
P. putida		
WCS358	Wild-type PGPR; SA$^-$ Psb$^+$	22
JM218	WCS358 Tn5 mutant; Psb$^-$	39
E. coli		
S17-1	*thi pro recA hsdR hsdM* RP4-2-Tc::Mu-Km::Tn7 Tp^r Sm^r	59
DH5α	*recA1 endA1* ϕ80d *lacZ dam-15*	Clontech
HB101	*pro leu thi lacY endA recA hsdR hsdM* Sm^r	10
Plasmids		
pLAFR1	pRK290 containing λ *cos* site; Tc^r Mob$^+$ Tra$^-$	21
pLAFR3	pLAFR1 plus multiple cloning site of pUC8	59
pJQ18	pSUP5011 derivative; carries Tn5-Mob-Tc	Alfred Pühler
pSUP2011	pBR325 replicon; Ap^r Cm^r Mob; Tn5 delivery plasmid	59
pRK2013	ColE1 replicon, helper plasmid; Km^r *tra*	20
pGEM-3Z	Cloning and transcription vector; Ap^r	Promega
pMB374-07	28-kb fragment from WCS374 cloned in pLAFR1; carries SA and pseudomonine synthesis genes	This work
p07H1	5-kb *Hin*dIII fragment from plasmid pMB374-07 cloned in pLAFR3	This work
p07E34	8.5-kb *Eco*RI fragment from plasmid pMB374-07 cloned in pLAFR3	This work
p07E3/p07E3R	5-kb *Eco*RI fragment containing *pmsCEAB* genes cloned in pLAFR3 in both orientations relative to *lacZ* promoter	This work
pE3/pE3R	5-kb *Eco*RI fragment containing *pmsCEAB* genes cloned in pGEM-3Z in both orientations relative to *lacZ* promoter	This work
pJMSal-10	pGEM-3Z with 0.7-kb *Eco*RI-*Pst*I fragment containing *pmsB* gene	This work
pJMSal-20	pGEM-3Z with 1.7-kb *Eco*RI-*Hin*dIII fragment containing *pmsAB* genes	This work
pLASal-10	pLAFR3 with 0.7-kb *Pst*I fragment containing *pmsB* gene	This work

Besides its siderophore activity, bacterial SA has an important role in inducing resistance in plants against pathogen infection. Thus, SA produced by the rhizobacterium *P. aeruginosa* 7NSK2 has been demonstrated to induce resistance against the fungal pathogen *Botrytis cinerea* on beans (17, 18). Likewise, heterologous expression of SA biosynthesis genes in *P. fluorescens* improves ISR in tobacco plants against tobacco necrosis virus (41). In plants, endogenous SA has a key role in systemic acquired resistance, an enhanced resistance status reached by a plant upon pathogen infection (63).

The route of SA biosynthesis in bacteria is not completely known. It has been suggested that in *M. smegmatis*, salicylate is derived from shikimate (49). Conversion of chorismate to isochorismate and subsequently to salicylate has been obtained from cell extracts of this microorganism (27, 38). Two genes responsible for SA biosynthesis in *P. aeruginosa* have been identified. The products of *pchB* and *pchA* genes have been proposed to catalyze the conversion of chorismate to salicylate via isochorismate (56). *P. fluorescens* WCS374 is a plant growth-promoting rhizobacterium (PGPR), originally isolated from the rhizosphere of potato (22), that produces SA and the green-fluorescent siderophore pseudobactin at low iron availability (33). Strain WCS374 suppresses *Fusarium* wilt in radish by ISR, and pseudobactin has been identified as one of the WCS374 traits involved in ISR (33). Likewise, these authors reported that other iron-regulated metabolites induce ISR in bioassays at low iron availability, which might be explained by SA production. However, they also suggested that additional siderophores may play a role in WCS374 ISR induction. The aim of this work was to localize and characterize the SA biosynthesis region of strain WCS374 as well as to identify additional siderophores produced by this strain under low iron availability. During the course of this investigation, evidence was obtained that SA biosynthesis in WCS374 is linked to the synthesis of a siderophore which has been chemically identified as pseudomonine.

MATERIALS AND METHODS

Strains, plasmids, and media. The bacterial strains and plasmids used are listed in Table 1. *Pseudomonas* strains were grown at 28°C in King's medium B (KB) (32), and *Escherichia coli* strains were grown at 30°C in Luria-Bertani medium (44). SA production was determined from cultures grown in standard succinate medium (SSM; pH 7.0) (42) for *Pseudomonas* strains and M9 minimal medium (53) for *E. coli* strains. All plasmids for sequencing were propagated in *E. coli* DH5α (Clontech) at 37°C. Antibiotics were added at the following concentrations (micrograms per milliliter) when required: ampicillin, 100; kanamycin (KAN), 50; nalidixic acid (NAL), 25; and tetracycline (TET), 20 (for *E. coli*) and 40 (for *Pseudomonas*).

DNA manipulations. Standard procedures were used for DNA electrophoresis, DNA transfer from agarose gels to nylon membranes (Boehringer Mannheim Biochemicals), preparation of competent cells, and transformation (53). Small-scale isolation of recombinant plasmids was done by alkaline lysis as described by Birnboim and Doly (9). Purification of plasmid DNA and elution of DNA restriction fragments from agarose gels were performed using Qiagen Inc. systems according to the instructions provided. DNA restrictions and ligations with T4 DNA ligase were conducted with enzymes purchased from Pharmacia according to the manufacturer's instructions. Hybridization was done with a nonradioactive detection kit from Boehringer Mannheim Biochemicals, and the chemiluminescence method was used to detect hybridization bands.

Tn*5* mutagenesis and bacterial matings. To perform random mutagenesis of *P. fluorescens* WCS374, the mobilization system of strain S17-1 and the suicide vector pSUP2011, carrying transposon Tn*5*, were used (59). Matings were carried out by mixing overnight cultures of donor strain S17-1 harboring pSUP2011 and recipient strain WCS374 in a ratio 1:1. After pelleting the cultures, the mating mixture was resuspended in a small volume (50 to 100 μl) and loaded onto a sterile Millipore filter (0.45-μm pore size) on KB agar plates. After 24 h of incubation at 28°C, cells were resuspended in fresh KB, and aliquots were plated on KB agar plates supplemented with KAN and NAL, to which WCS374 is intrinsically resistant. To avoid counterselection of mutants affected in iron uptake and metabolism, 100 μM $FeCl_3 \cdot 6H_2O$ was added to the selection medium. The transposition frequency in these experiments was 10^{-5} per recipient cell. Km^r colonies were then screened for lack of fluorescence under UV irradiation on KB agar plates, growth on KB agar plates amended with 800 μM 2,2-bipyridyl (BDH) (which acts as an iron chelator) (39), growth on SSM agar plates, and inability to produce orange halos on chrome azurol S (CAS) medium agar plates (55). The presence of single transposition events in siderophore-deficient mutants was checked by hybridization. Total DNA from the Km^r mutants was isolated, digested with *Eco*RI, blotted onto a membrane, and hybridized against the digoxigenin-labeled internal *Hin*dIII fragment of Tn*5*, using high-stringency conditions.

Generation of a second Tn*5* insertion in SA^- Pms^- mutant 374-05 was performed using the system based on the suicide vector pJQ18 (28), which carries a modified Tn*5* (Mob Tc^r). Km^r and Tc^r colonies were isolated from matings using S17-1 harboring pJQ18 as the donor strain and mutant 374-05 as the recipient. Southern blots and DNA-DNA hybridization experiments were conducted to reveal the presence of two Tn*5* insertions.

Transfer of the WCS374 gene library (see below) from *E. coli* DH5α to strain JM218, a pseudobactin-deficient Tn*5* mutant derived from *P. putida* WCS358 (39), was carried out in triparental matings using the helper plasmid pRK2013 (20).

Siderophore determination. Siderophore production by bacterial strains was detected by using the universal siderophore detection medium CAS agar (55). A siderophore producer colony chelates iron from the medium, and a shift from blue (chelated CAS) to orange (unchelated CAS) is obtained. Droplets (3 μl) of an overnight SSM culture were spotted on plates, and after incubation (1 to 3 days, at 28 or 37°C) the relative halo size ([halo diameter − colony diameter]/halo diameter]) was determined. Halo determination was done in triplicate and repeated at least three times.

Presence of catechol and hydroxamate groups in supernatants of bacterial cultures grown for 48 to 64 h in SSM was determined as described by Arnow (4) or Rioux et al. (52) and Csáky (15), respectively. Pyochelin detection was performed following the procedure described by Cox and Graham (13).

(i) In vitro SA production. SA production from culture supernatants was determined as previously described (33, 43). Strains of *Pseudomonas* spp. were grown in liquid SSM at 28°C; *E. coli* strains were grown in M9 medium at 30°C. After removal of cells by centrifugation, culture supernatants were acidified with 1 N HCl to pH 2, and SA was extracted into $CHCl_3$ upon vigorous shaking (culture supernatant:$CHCl_3$, 1:1). For low levels of SA production, 1 volume of $CHCl_3$ was used to extract SA from up to 3 volumes of spent medium. An absorbance spectrum (200 to 400 nm) of the organic phase was determined to obtain a qualitative determination. For quantitative measurements, 1 volume of H_2O and 1.25×10^{-3} volumes of 2 M $FeCl_3 \cdot 6H_2O$ were added to the $CHCl_3$ phase. The absorbance of the purple iron-SA complex developed in the aqueous phase was measured at 527 nm, using SA dissolved in the growth medium and treated as described above as a standard.

(ii) Purification and identification of the siderophore pseudomonine. A lyophilized culture filtrate of *P. fluorescens* WCS374-08, grown in liquid SSM, was redissolved in water to a concentration of 100 mg/ml; 1 ml of this solution was applied to an Alltech C18 reversed-phase solid extraction column (5 ml), conditioned by washing with 5 ml of 100% acetonitrile (ACN), 5 ml of 40% ACN, and 5 ml of H_2O. After the sample solution was applied, the column was washed four times with 5 ml of H_2O. The pseudomonine was eluted with 1 ml of 40% ACN followed by 1 ml of 100% ACN. Both fractions were shown to contain pseudomonine, and both were lyophilized. The pseudomonine eluted in 100% ACN was redissolved in 50 μl of 5% acetic acid (AcOH), and 2 μl was loaded into the glycerol matrix for fast atom bombardment (FAB) mass spectroscopy and collision-induced dissociation (CID) analysis. The pseudomonine eluted in 40% aqueous ACN was redissolved in 50 μl of ethanol, and approxiamtely 10 μl was analyzed by probe electron ionization (EI). For H-D exchange, the fraction was redissolved in 100 μl 5% deuterated AcOH, and 2 μl was loaded into a D-glycerol matrix.

FAB mass spectra were obtained in the positive mode using a JEOL JMS-SX/SX102A tandem mass spectrometer using 10-kV accelerating voltage. The FAB gun was operated at 6 kV with an emission current of 10 mA, using xenon as the bombarding gas. Spectra were scanned at a speed of 30 s for the full mass range specified by the accelerating voltage used and then recorded and processed on a Hewlett-Packard HP9000 series data system using the JEOL Complement software. CID mass spectra were obtained on the same instrument, using helium as the collision gas in the third field free region at a pressure sufficient to reduce the parent ion to one-half of its original intensity.

EI spectra were obtained in the positive mode on a JEOL AX505 mass spectrometer operated at 3-kV accelerating voltage and with an ionizing beam of 70 eV. The sample was introduced using a direct probe, which was heated for 1 min at 30°C and then heated to a final temperature of 350°C at a rate of 64°C min^{-1}. Spectra were scanned from *m*/*z* 10 to 800 in 3 s and recorded and processed on a Hewlett-Packard HP9000 series data system using the JEOL Complement software.

The nuclear magnetic resonance (NMR) spectra were recorded on a Bruker AMX600 spectrometer operating at 600.13 MHz for ^1H and 150.9 MHz for ^{13}C.

Construction of a gene library and cloning of SA biosynthesis genes. Genomic WCS374 DNA was isolated and partially digested with *Eco*RI. Sucrose gradient fractionation, agarose gel electrophoresis for size analysis, fragment DNA preparation, and ligation reaction with *Eco*RI-digested cosmid vector pLAFR1 were performed as described by Sambrook et al. (53). In vitro packaging and transduction of the ligated DNA were performed as instructed by the manufacturer (Boehringer Mannheim Biochemicals).

Deletion analysis of the SA biosynthesis region and DNA sequencing. The region involved in SA biosynthesis in *P. fluorescens* WCS374 was mapped by subcloning and deletion analysis of plasmid pMB374-07 (Fig. 1). The 5-kb *Eco*RI fragment from pMB374-07 containing the SA biosynthesis region was subcloned in pGEM-3Z (Promega) in both orientations with respect to the *lacZ* promoter, yielding plasmids pE3 and pE3R. Plasmid DNAs were digested using the single *Xba*I and *Sma*I sites present in the multiple cloning site of pGEM-3Z. *Xba*I was used to generate 5′ protruding ends which were protected from exonuclease III digestion with α-phosphorothioate-derived deoxynucleoside triphosphates (dNTPs) plus Klenow enzyme. Subsequently, *Sma*I was used to generate blunt ends susceptible to exonuclease III digestion. Templates were generated by progressive unidirectional deletions using the Erase-a-Base system from Promega Corporation according to the manufacturer's instructions. The resulting fragments were ligated and transformed into DH5α cells. Plasmids from ampicillin-resistant transformants with suitable deletions were selected, purified using a Qiagen kit, and used for DNA sequencing. Selected deletion plasmids were screened for the ability to direct SA biosynthesis in *E. coli* as described above.

DNA sequencing was performed on both strands in overlapping fashion. The DNA sequence of the 5,057 bp was determined using an Applied Biosystems model 373A automated DNA sequencer (Hubrecht Laboratorium, Utrecht, The Netherlands). When necessary, specific oligonucleotides synthesized by Pharmacia Biotech were used as primers for sequencing gaps. Sequence analysis and homology search were done with Genepro version 4.0 (Riverside Scientific Enterprises) and the BLAST programs (1) at the National Center for Biotechnology Information network service.

Use of RT-PCR to study *pms* gene expression. Expression of *pms* genes in cultures under low- and high-iron conditions was studied in reverse transcriptase-mediated PCR (RT-PCR) experiments. We used mutant 374-08 as an internal gene expression control since it contains the neomycin phosphotransferase gene (*neo*) (7). This gene, carried by the Tn*5* element present in this mutant, is expressed when KAN is present in the incubation medium, and its expression can be compared to that of the *pms* genes. Total RNA was isolated from strains WCS358 (used as a negative control for SA production), WCS374, and 374-08 with a Qiagen RNeasy kit according to the manufacturer's instructions. Bacteria were grown in liquid SSM (15 ml) for at least 48 h at 28°C. For high-iron conditions, cells from 48-h-old cultures were spun down and resuspended in 15-ml of fresh SSM, amended with 100 μM $FeCl_3 . 6H_2O$. The cells were then incubated for 3 h at 28°C; 10^9 cells from low- and high-iron cultures were used for total RNA isolation. RNA was eluted in 50 μl of pyrocarbonic acid diethyl ester (DEPC)-treated water. RNA concentration and quality were determined spectrophotometrically and by gel electrophoresis, respectively. To exclude the possibility of contamination with traces of DNA, RNA samples were treated with 20 U of RNase-free DNase (Pharmacia Biotech) for 30 min at 37°C. RNAs were subsequently purified by the method described in the RNeasy kit for RNA cleanup. Simultaneously, DNA samples of strain WCS374 and mutant 374-08 (2 μg of genomic DNA in 50 μl of DEPC-treated water) were treated with RNase-free DNase, as controls to check the effectiveness of the DNase treatment.

cDNA synthesis was carried out using a First-Strand cDNA Synthesis kit

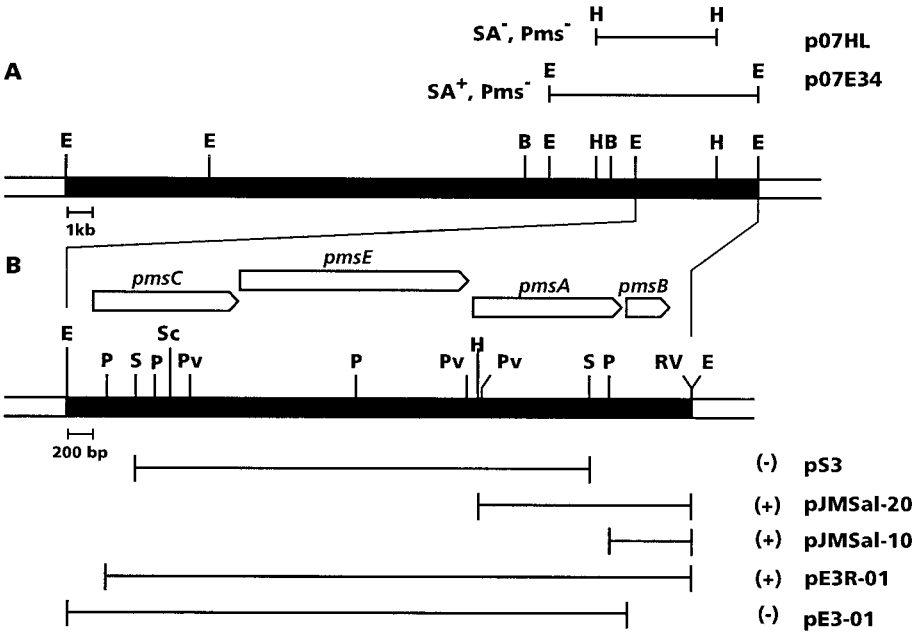

FIG. 1. (A) Restriction map of the 28-kb insert cloned in plasmid pMB374-07. The two lines above the restriction map represent subclones which showed the phenotypes indicated (SA^- and/or Pms^-) when harbored by JM218. (B) Physical map of the minimal 5-kb *Eco*RI fragment responsible for SA biosynthesis. Lines below the restriction map represent different deletion clones and subclones constructed to delimit the minimal region involved in SA biosynthesis in *E. coli*. Production [(+)] or nonproduction [(−)] of SA is indicated. Restriction sites: E, *Eco*RI; B, *Bam*HI; H, *Hin*dIII; S, *Sal*I; Sc, *Sac*I; Pv, *Pvu*II; RV, *Eco*RV.

(Pharmacia Biotech); 2.5 μg of total RNA was used. The RNA samples were brought to 20 μl with DEPC-treated water and heated at 65°C for 10 min. The reaction mixtures (final volume of 33 μl) consisted of 1 μl of 200 mM dithiothreitol, 1 μl of the appropriate primer (20 pmol), 11 μl of the Bulk First-Strand cDNA reaction mix provided by the kit (murine reverse transcriptase, RNAguard, RNase- and DNase-free bovine serum albumin, and dNTPs in aqueous buffer), and the heat-denatured RNA. After mixing, samples were incubated at 37°C for 1 h. For cDNA synthesis of the *pms* gene transcript, primer SAL03 (5′-CAATGCAGGATTTGCTGTTG-3′, corresponding to nucleotides 4805 to 4786) was used. For cDNA synthesis of the *neo* mRNA in 374-08, primer KM03 (5′-CACCATGATATTCGGCAAGC-3′, corresponding to nucleotides 2144 to 2125)(10) was used. For PCRs, 1 μl of the cDNA reaction mixture, consisting of 1.25 mM $MgCl_2$, 10 mM Tris-HCl (pH 8.3), 50 mM KCl, 0.5 U of Ampli-*Taq* DNA polymerase (Perkin-Elmer), 2 μl of dNTP mixture (2.5 mM each), 1.5 μl of appropriate primers (10 pmol), and water to a final volume of 25 μl, was used. Amplification was performed in an Amplitron II (Thermolyne) apparatus, setting the samples at 92°C for 4 min, followed by 30 cycles at 92°C for 30 s, 56°C for 30 s, and 72°C for 30 s. The following pairs of primers were used: for *pmsB* intragenic cDNA amplification, SAL01 (5′-GAACCTCAATGACATTCGAG-3′, corresponding to nucleotides 4548 to 4567) and SAL02 (5′-GTAGAGCTT CTCGACGAAAG-3′, corresponding to nucleotides 4742 to 4761) (product, 214 bp); for the *pmsAB* region, HDC01 (5′-CGCCATCGAATCAAACACAG-3′, positions 4163 to 4182) and SAL02 (product, 599 bp); for the *pmsCE* region, DHB01 (5′-GAATGGGTCGTAACGATTCG-3′, positions 1224 to 1243) and DHB02 (5′-ATATTGGGCAACTGCACCAG-3′, positions 1662 to 1643) (product, 439 bp); and for the *neo* region, KM01 (5′-GACAATCGGCTGCTCTGA TG-3′, positions 1631 to 1650) and KM02 (5′-TGCTCTTCGTCCAGATCATC-3′, positions 2035 to 2016) (10) (product, 405 bp).

Nucleotide sequence accession number. The nucleotide sequence of the *P. fluorescens* WCS374 *pmsCEAB* genes has been deposited in the EMBL, GenBank, and DDBJ nucleotide sequence databases under accession number Y09356.

RESULTS

***P. fluorescens* WCS374 produces three siderophores at low iron availability.** To obtain mutants impaired in siderophore production, random Tn*5* mutagenesis of *P. fluorescens* strain WCS374 was carried out. Upon screening of some 4,000 Km^r colonies, 13 nonfluorescent (deficient in production of pseudobactin [Psb-deficient]) mutants on KB agar plates were isolated. However, all of the mutants were still able to grow on KB supplemented with 2,2-bipyridyl. This result could be explained either by the production of SA, which can act as a siderophore, or by the presence of third siderophore other than pseudobactin and SA in strain WCS374.

CAS medium (55) was used to assess the presence of siderophore activity in the Psb-deficient mutants isolated. The mutants tested were still able to produce an orange halo on CAS medium agar plates similar in size to the one produced by wild-type WCS374. Moreover, no significant differences in relative halo size were encountered after 48 h of incubation at two different temperatures: 28°C, optimal for growth of the strains, and 37°C, which is repressive for pseudobactin production (39). Finally, the presence of a single Tn*5* insertion was confirmed by hybridization. All mutants studied contained a unique insertion (data not shown).

All of the Psb-deficient mutants analyzed produced comparable quantities of SA; however, production was significantly lower than for WCS374 (Table 2). Nevertheless, SA produced by WCS374 or the Psb-deficient mutants could not explain the siderophore activity detected in the CAS assay, since SA can induce a transitory color shift on CAS medium agar plates only when applied at high concentrations (data not shown). Interestingly, SSM cultures of Psb-deficient mutants emitted a blue fluorescence under UV irradiation. This attribute facilitated the differentiation between pseudobactin producers (green fluorescence), Psb-deficient mutants (blue fluorescence), and the double mutants (nonfluorescent) described below.

The normal growth abilities displayed under low-iron con-

TABLE 2. SA production in SSM by different *Pseudomonas* strains (assay A) and in M9 medium by *E. coli* DH5α harboring different plasmids constructed in this work (assay B)

Strain	SA (μg/ml)
Assay A	
WCS374	54 ± 25
374-05	ND[a]
374-05.1	ND
374-08[b]	14 ± 5
JM218(pLAFR1/pLAFR3)	ND
JM218(pMB374-07)	3.2 ± 1.2
JM218(p07E3R)	19 ± 7
JM218(p07E3)	3.2 ± 0.7
Assay B	
DH5α	ND
DH5α(pE3)	41 ± 18
DH5α(pE3R)	61 ± 6
DH5α(pE3-01)	ND
DH5α(pE3R-01)	7.2 ± 1.3
DH5α(pJMSal-10)	8.8 ± 2.7
DH5α(pJMSal-20)	8.9 ± 4.6

[a] ND, not detected.
[b] Selected as representative of the WCS374 Psb$^-$ mutants.

ditions by the Psb-deficient mutants along with the capacity to induce wild-type siderophore activity in CAS medium agar plates, which can be discriminated by different incubation temperatures, indicated the presence of an additional siderophore other than SA and pseudobactin produced by strain WCS374.

Identification of a mutant impaired in production of both SA and a newly detected siderophore and construction of SA$^-$ Psb-deficient mutants. During the screening for Psb-deficient mutants, a mutant (374-05) showing enhanced production of pseudobactin compared to that by *P. fluorescens* WCS374 was also isolated. When analyzed for SA production, the result was negative (Table 2). The results obtained in the CAS medium agar assay revealed that the halo produced at 28°C was not significantly different from the one produced by WCS374 or the Psb-deficient mutants. However, incubation at 37°C showed a strong reduction of the relative halo size, due to repression of pseudobactin synthesis at this temperature (39). Actually, pseudobactin was masking the detection of the additional siderophore in CAS agar plates. In contrast, no reduction in halo size at 37°C was observed for the Psb-deficient mutant 374-08. This observation indicated that mutant 374-05 was impaired in the production of not only SA but also the unidentified siderophore. Yet, siderophore activity was detectable in mutant 374-05 at 37°C.

These results, along with the facts that some bacteria, including *Pseudomonas* spp., produce more than one siderophore and that SA is a precursor in the biosynthesis of certain siderophores, led us to hypothesize that production of SA and the blue-fluorescent siderophore in strain WCS374 are related. Psb-deficient mutants were derived from mutant 374-05 to investigate whether the SA$^-$ phenotype in 374-05 is coupled to siderophore deficiency. The suicide vector system pJQ18 (28) was used to generate a second Tn*5* insertion in mutant 374-05. Double mutants were selected on the basis of both Km^r and Tc^r. The transposition frequency was lower than that obtained in the first mutagenesis, in accordance with the previously described phenomenon of inhibition of transposition exerted by a preexisting Tn*5* in the cell (8). After screening of some 900 clones, three Km^r and Tc^r, Psb-deficient (nonfluorescent) colonies with significantly reduced halos in CAS medium were isolated. Moreover, the three mutants (374-05.1, 374-05.8, and 374-05.10) did not show the characteristic blue fluorescence of Psb-deficient mutants in SSM cultures, and as for the parent strain 374-05, SA production was not detectable. This result further supported the link between SA and the unidentified siderophore in WCS374. DNA-DNA hybridization experiments revealed the presence of two bands that hybridized with digoxigenin-labeled Tn*5* DNA (data not shown).

Identification of the additional siderophore as the SA-based siderophore pseudomonine. Attempts to identify pyochelin, an SA-based siderophore, in culture supernatants of the strains tested failed. Moreover, neither catechol nor hydroxamate groups were detected in the supernatant of these strains. In contrast, weak positive reactions for both were obtained in pseudobactin producer strains WCS374 and 374-05. This can be explained by the presence of these groups in the structure of this siderophore (26). To identify the siderophore produced by WCS374, culture supernatants of mutant strain 374-08 grown in liquid SSM were used.

(i) Mass spectrometric analysis of pseudomonine. The siderophore preparation was analyzed in the positive-ion mode using FAB mass spectrometry and CID, as well as EI. In both the positive-ion mode FAB mass spectrum recorded from the siderophore isolated in this study and the (unpublished) positive-ion mode FAB mass spectrum recorded by Anthoni and coworkers from pseudomonine (3), a protonated molecule was observed at *m/z* 331. To obtain structural information, the ion at *m/z* 331 was submitted to CID tandem mass spectrometry (Fig. 2A). The most abundant fragment ion is observed at *m/z* 211 and corresponds to the loss of the SA group (Fig. 2B). The SA group fragment is observed at *m/z* 121. The ion at *m/z* 110 corresponds to a histidine immonium ion, which is derived from the histamine moiety, while the ions at *m/z* 82 and 95 also arise by cleavage of the hydrocarbon backbone of the histamine moiety. The ion at *m/z* 138 corresponds to cleavage in the cyclothreonine moiety with charge retention on the histamine-containing part of molecule. We assign the ion at *m/z* 204 as deriving from the SA-containing portion of the molecule and being generated by cleavage in the cyclothreonine moiety. This ion is complemented by an ion at *m/z* 128 that we assign as arising via an analogous cleavage in the cyclothreonine moiety, but now with charge retention on the histamine-containing part of the molecule.

To further verify these assignments, pseudomonine was submitted to H-D exchange and subsequent mass spectrometric analysis. In the FAB mass spectrum, this time recorded in a deuterated glycerol matrix, the pseudomolecular ion shifted by 4 atomic mass units to *m/z* 335, which is in correspondence with the replacement of three exchangeable protons by deuterium and one deuterium carrying the charge. The CID mass spectrum of the ion at *m/z* 335 confirmed the assignment of the fragmentation described above, with all fragments indeed incorporating the expected number of D atoms. Figure 2B shows the ions observed in the CID spectrum of the deuterated species and the exchangeable hydrogens.

The EI mass spectrum (data not shown) is directly comparable to the unpublished EI spectrum recorded by Anthoni et

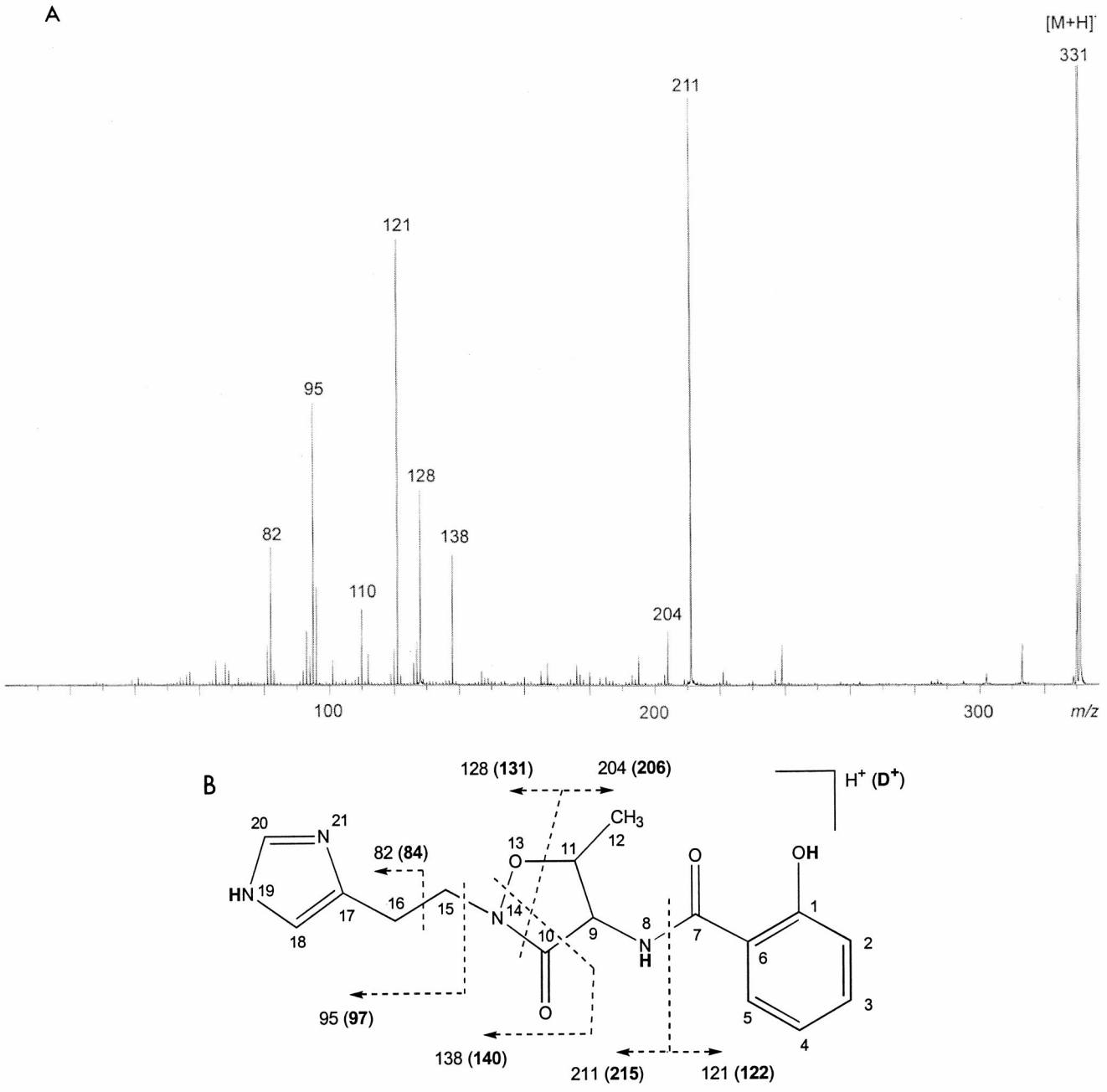

FIG. 2. (A) CID mass spectrum of the compound found in the fraction eluting in 100% ACN. (B) Fragmentation scheme for the component with $[M + H]^+$ at *m/z* 331. Boldface numbers indicate fragment masses of the ions obtained from the deuterated component. Small numbers refer to the atom numbering used to assign the NMR data summarized in Table 3. The H atoms shown in boldface correspond to exchangeable protons.

al. (3). The molecular ion is observed at *m/z* 330, and fragment ions are observed at *m/z* 82, 95, 110, 121, 127, 138, and 204, corresponding to the fragment ions that were observed in the CID spectrum (see above).

(ii) NMR analysis of pseudomonine. To obtain further structural information from the bioactive compound isolated, the fraction containing the bioactive compound was analyzed by ^{13}C and ^{1}H NMR. The chemical shifts are summarized in Table 3, alongside the NMR data obtained by Anthoni et al. (3). A comparison of the two data sets makes it clear that the chemical shifts observed by both groups are nearly identical.

SA and pseudomonine biosynthesis loci are linked in the strain WCS374 genome: delimitation of the SA biosynthesis region. To localize a recombinant cosmid clone harboring the biosynthetic regions of SA and pseudomonine, heterologous expression was pursued. JM218, a Tn*5* Psb-deficient mutant of *P. putida* WCS358 (39), produces a very small halo on CAS medium agar plates. Both WCS358 (33) and JM218 (Table 2) do not produce SA. Thus, halo restoration could be used as a marker for expression of WCS374 siderophore biosynthetic genes in JM218. Matings were performed using a mixture of the gene library (>8,000 clones; average insert size, 20 kb) in

TABLE 3. ^{13}C and ^{1}H NMR data obtained on pseudomonine[a]

Position	δ_C		δ_H	
	This study	Reference 3	This study	Reference 3
1	161 (?)	161.1		
2	116.8	118.5	6.93	6.92
3	132.8	135.3	7.41	7.40
4	117.1	120.3	6.89	6.90
5	127.1	129.1	7.83	7.78
6		116.5		
7		171.1		
9	57.1	59.5	4.79	4.62
10	166.8	169.1		
11	78.4	79.9	4.50	4.45
12	15.1	17.2	1.51	1.46
15	44.1	45.1	3.98, 3.88	3.99, 3.89
16	23.2	23.6	3.02, 2.99	3.10
17		132.6		
18	116.3	118.2	6.98	7.38
20	134.2	135.3	7.64	8.62

[a] Recorded in CD_3OD; chemical shifts relative to 3.35 ppm for ^{1}H and 47.07 ppm for ^{13}C. Atom numbering is according to Fig. 1 of reference 3 and Fig. 2B.

DH5α as donor strain and JM218 as recipient strain. Helper plasmid pRK2013 (20) was used to aid transfer of the recombinant cosmids. Selection of the transconjugants was made on KB without Mg^{2+} (to avoid antagonism with TET), supplemented with TET, KAN, and NAL. After screening 2,150 Tc^r and Km^r JM218 transconjugants, we isolated 36 clones capable of inducing halo production in CAS medium agar plates. Only those clones that showed halos not only at 28°C but also at 37°C, where pseudobactin synthesis is repressed (39), were selected. The three clones that fulfilled this criterion (pMB374-07, pMB374-15, and pMB374-31) were also the only ones showing SA production. However, the amount of SA detected was far lower than that obtained for WCS374 (33) (Table 2). SSM culture supernatants of JM218 carrying these recombinant clones showed a blue fluorescence under UV light, which corroborates the observation obtained for the Psb-deficient mutants of WCS374. High-pressure liquid chromatography (HPLC) analysis of the culture supernatant of JM218 carrying pMB374-07 revealed the presence of pseudomonine (data not shown).

According to their *Eco*RI restriction patterns, the three clones isolated were identical. The insert, with a calculated size of 28 kb, consisted of four fragments of 14, 5.5, 5, and 3.5 kb. A restriction map of plasmid pMB374-07, used in further experiments, is shown in Fig. 1. Subcloning of the different restriction fragments led us to identify the minimal region involved in SA biosynthesis in WCS374 (Fig. 1). A 5-kb *Eco*RI fragment was sufficient to promote SA synthesis in *P. putida* JM218 (plasmids p07E3 and p07E3R) and *E. coli* strains (plasmids pE3 and pE3R) (Table 2). Higher SA levels were obtained for plasmid p07E3R than for plasmid pMB374-07. Plasmids containing only the 5-kb *Eco*RI fragment were no longer able to induce halo production by JM218 on CAS medium agar plates; only JM218 carrying the entire, originally isolated cosmid pMB374-07 retained this ability. Additionally, the characteristic blue fluorescence detected in the SSM supernatant of JM218(pMB374-07) cultures was weaker for JM218(p07E3R), despite the higher SA levels detected for the latter (Table 2).

These results support the hypothesis that SA and pseudomine production are linked in strain WCS374. There was a correlation among halo production on CAS medium agar plates and the blue fluorescence displayed by Psb-deficient mutants in SSM. Moreover, all pseudomonine-producing strains showed the ability to synthesize SA, and plasmid pMB374-07 contains closely linked genes for the biosynthesis of both compounds.

Nucleotide sequence analysis of the SA biosynthesis region. Nucleotide sequence analysis of the 5,057-bp *Eco*RI fragment (56.48% G+C content) revealed the presence of four major open reading frames (ORFs) with high coding probability and rightward polarity (Fig. 1). The first ORF (ORFA) is preceded by a strong potential ribosome binding sequence (RBS) (GGA GG) that matches the consensus RBS of *E. coli* (58).

ORFA is 1,176 bp long (positions 207 to 1382), potentially coding for a 391-amino-acid-residue-long protein. A second ORF (ORFB), identified between positions 1409 to 3244, is 1,836 bp long and codes for a putative protein of 611 amino acid residues. At 39 bp downstream from the TGA stop codon of ORFB is found a third ORF (ORFC), 1,218 bp long, potentially coding for a 405-amino-acid-residue protein (positions 3284 to 4501). A strong RBS (AAGGAG) is found at 6 bp upstream from the ATG starting codon. Finally, at 14 bp from the TGA stop codon of ORFC, the ATG start codon of ORFD (positions 4516 to 4851) was located. It was only 336 bp long, with a predicted translation product of 111 amino acid residues. An appropriate RBS (AAGAGA) was found at positions 4502 to 4507. The four ORFs identified in the 5-kb region are closely connected, supporting the idea of a polycistronic organization.

Protein sequence homology. A search in the databases for protein homology yielded relevant data for all predicted translational products of the sequenced region. ORFA (proposed name *pmsC*, for pseudomonine synthesis) codes for a protein with a predicted molecular weight of 43,102. The deduced amino acid sequence showed similarities with several chorismate-utilizing enzymes: isochorismate synthases (ICSs) of *E. coli* (EntC; EMBL/Swiss-Prot accession number P10377; 45% identity and 73% similarity), *Aeromonas hydrophila* (AmoA; P23300; 43% identity and 69% similarity), *Vibrio cholerae* (VibC; 007898; 43% identity and 69% similarity), *Bacillus subtilis* (DhbC; P45744; 40% identity and 71% similarity), and *P. aeruginosa* (PchA; Q51508; 38.5% identity and 52.6% similarity in 192 residues of the carboxy-terminal domain). It also showed moderate homology with menaquinone-specific ICS (MenF) from different bacteria and weak homology with component I of anthranilate synthases (TrpE) and *p*-aminobenzoate synthase component I (PabB) from different organisms. ICS catalyzes the conversion of chorismate to isochorismate. This compound is utilized for the biosynthesis of some quinones and phenolic acid derivatives such as 2,3-dihydroxybenzoic acid (2,3-DHB). ICSs cited above have been reported as key enzymes in the biosynthetic pathway of siderophores such as enterobactin (19), pyochelin and SA (56), amonabactin (6), and vibriobactin (O07898).

The deduced amino acid sequence of ORFB (*pmsE*) (predicted molecular weight of 67,417) also showed strong similarities with proteins involved in siderophore synthesis: 2,3-dihydroxybenzoate-AMP ligase of *E. coli* (EntE; P10378; 55% identity and 81% similarity) and *B. subtilis* (DhbE; P40871; 49.7% identity and 70% similarity in 463) for enterobactin

synthesis, vibriobactin (VibE; O07899) biosynthesis of *V. cholerae* (45% identity and 74% similarity), pyochelin (PchD; P72175) biosynthesis of *P. aeruginosa* (43% identity and 71% similarity), and yersiniabactin (YbtE; Q56950) biosynthesis of *Yersinia pestis* (39% identity and 70% similarity). The function of EntE is the activation of the carboxylate group of 2,3-DHB, via an ATP-dependent PP_i-exchange reaction. It is one of the constituents of a membrane-bound multienzyme complex (35). Moderate to weak homologies were found with other enzymes that act via an ATP-dependent covalent binding of AMP to their substrates, such as 4-coumarate coenzyme A ligase, surfactin synthetase subunit 1, and luciferin 4-monooxygenase (luciferase).

The ORFC (*pmsA*) translational product (predicted molecular weight of 45,726) showed high homology with pyridoxal phosphate (pyridoxal-P)-dependent histidine decarboxylases (HDC) from *Klebsiella planticola* (P28578; 77% identity), *Morganella morganii* (P05034; 76% identity), *Enterobacter aerogenes* (P28577; 75% identity), and *Vibrio anguillarum* (Q56581; 62% identity). Moreover, 39% identity and 72% similarity were also found with HDC of tomato (*Lycopersicum esculentum*) (P54772). Important features such as the sequence SXHK (positions 231 to 234), found in other pyridoxal-P-dependent carboxylases, the lysine residue that binds the molecule of pyridoxal-P (position 234), and the serine residue (position 324) that binds the adduct formed between pyridoxal-P and the inhibitor α-fluoromethylhistidine (25) are also present in the WCS374-encoded HDC. However, a common nucleotide sequence found upstream of *hdc* genes from *M. morganii, K. planticola* and *E. aerogenes*, and postulated to be a histidine-responsive element (30), was not detected upstream of the putative *hdc* gene of strain WCS374. HDC catalyzes decarboxylation of histidine to histamine. Although histamine production has been reported for different pseudomonads (23), this is to our knowledge the first putative *hdc* gene sequenced for a *Pseudomonas* species. Histamine has been found in the molecular structures of different siderophores: anguibactin from *V. anguillarum* (29), pseudomonine from *P. fluorescens* AH2 (3), and acinetobactin from *Acinetobacter baumannii* (65). It has been shown by mutation analysis that the *hdc* gene is essential for the biosynthesis of anguibactin (62).

Comparison of the ORFD (*pmsB*) amino acid sequence (predicted molecular size of 13,003 Da) with database entries revealed significant homology to an unknown ORF of *V. vulnificus* (P74964; 60% identity and 83% similarity) and to the salicylate biosynthesis protein PchB of *P. aeruginosa* (56) (57% identity and 69% similarity). It has been hypothesized that PchB has isochorismate-pyruvate lyase activity. PchB together with PchA (a putative isochorismate synthase) are required for SA synthesis in *P. aeruginosa*. Interestingly, PmsB showed similarity to the bifunctional TyrA proteins (chorismate mutase/prephenate dehydrogenase; T protein) of *Haemophilus influenzae* (P43902), *Erwinia herbicola* (Q02287), and *E. coli* (P07023). The homology was located in the N-terminal domain of TyrA. TyrA proteins are larger than FbsB, and no homology was found with the monofunctional chorismate mutase from *B. subtilis* (24), the smallest natural chorismate mutase known (127 amino acids), and similar in size to FbsB (111 residues). However, lack of sequence homology between chorismate mutases of different species is well known (48).

Expression of SA genes in *E. coli*. SA was detected in M9 culture supernatants of *E. coli* DH5α cells carrying plasmid pE3 or pE3R (Table 2), suggesting that the putative promoter detected upstream of *pmsC* is functional in *E. coli*. Although high SA levels were detected, irrespective of orientation, enhanced SA production was obtained when the genes were properly oriented with regard to the *lacZ* promoter present in pGEM-3Z (pE3R). SA was also detectable in the spent medium of DH5α cells harboring different deletion clones, as well as subclones (Table 2). Deletions affecting *pmsB* (plasmid pE3-01) (Fig. 1) failed to produce SA in DH5α, indicating that this gene is essential for SA biosynthesis. Deletions affecting genes upstream of *pmsB* (i.e., plasmid pE3R-01 [Fig. 1], a 233-bp deletion derivative affecting the potential promoter region and the first nine codons of *pmsC*) resulted in 10-fold-lower SA production (Table 2). Likewise, DH5α carrying plasmids pJMSal-10 and pJMSal-20 produced detectable amounts of SA (Table 2).

Expression of *pms* genes is iron regulated. DNA sequence analysis identified putative σ^{70} promoter sequences only upstream of *pmsC*, suggesting that *pms* genes might have a polycistronic organization. The presence of two potential Fur boxes suggests that expression of the *pms* genes is iron regulated. Expression of *pms* genes was analyzed by RT-PCR. Total RNA from strains WCS374 and 374-08 grown in SSM was used for cDNA synthesis using primer SAL03. For subsequent PCR experiments, we used several pairs of primers that overlapped different *pms* genes: SAL01-SAL02 to define an internal *pmsB* PCR product, HDC01-SAL02 to yield a PCR product spanning *pmsAB*, and DHB01-DHB02 to amplify a fragment that partially overlaps the *pmsCE* coding region (Fig. 3A). For cDNA synthesis from *neo* mRNA, primer KM03 was used. The internal primer pair KM01-KM02 was used for PCR. If a polycistronic mRNA is obtained from the cDNA synthesis using primer SAL03, the predicted PCR products will be detected in all primer combinations designed. The result of this experiment is shown in Fig. 3B. PCR products expected for SAL01-SAL02 (214 bp), HDC01-SAL02 (599 bp), and DHB01-DHB02 (439 bp) were detected in mutant 374-08 and WCS374 cDNA PCRs. Similarly, the PCR product predicted for KM01-KM02 (405 bp) was detected in mutant 374-08 cDNA but not in WCS374 cDNA. The band sizes were concordant with PCR products obtained in PCR control reactions using WCS374 and 384-08 genomic DNAs as templates. Simultaneously, control PCRs of genomic DNA treated with RNase-free DNase did not yield any product, indicating that PCR bands due to DNA contamination in RNA samples can be excluded.

RT-PCR experiments also confirmed that expression of *pmsCEAB* genes is repressed by iron. When WCS374 and 374-08 were incubated during 3 h in SSM amended with 100 μM $FeCl_3$, a strong reduction of *pmsCEAB* transcript, measured as the corresponding PCR products, was observed (Fig. 3B and C), whereas *neo* gene expression in mutant 374-08 was not affected by iron. A semiquantitative determination of transcript repression was calculated on the basis of dilution series of the cDNA sample used in PCRs. PCR products from cDNA samples of cultures grown under high-iron conditions were approximately 100-fold lower than those from low-iron condi-

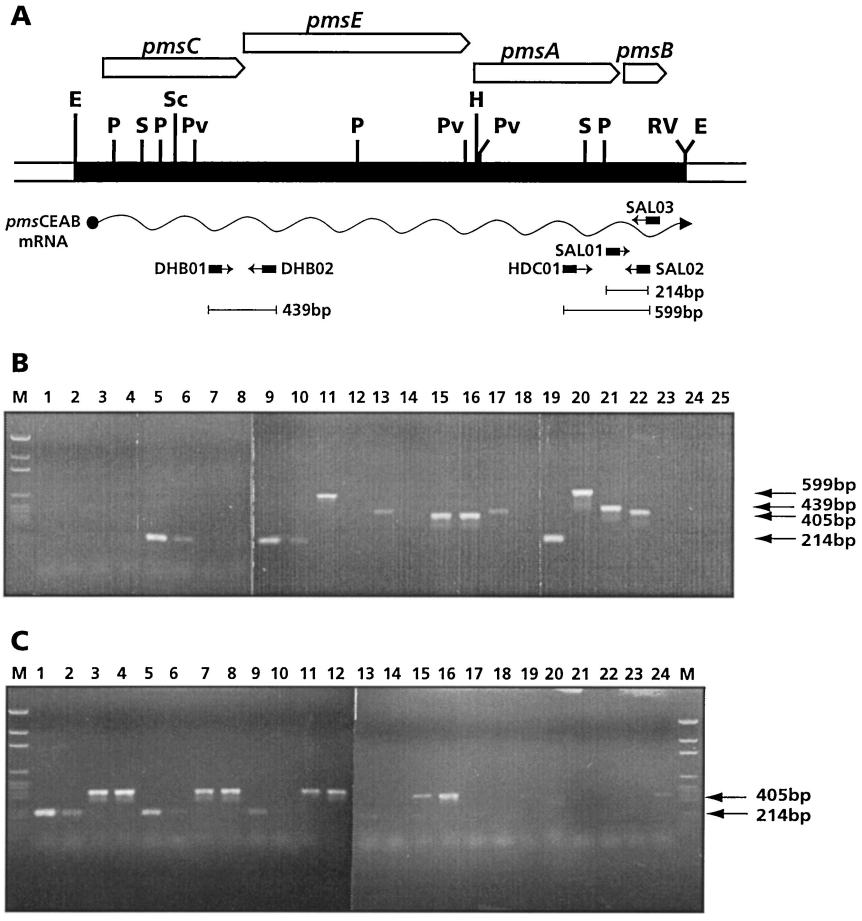

FIG. 3. Analysis of *pms* gene expression by RT-PCR. (A) Scheme representing positions of the primers used in this study, as well as lengths of the expected PCR products. Restriction sites are abbreviated as in Fig. 1. (B) RT-PCR products obtained from cDNA samples obtained after total RNA isolation of bacterial cultures grown under low- and high (Fe^{3+})-iron conditions. Experiments were performed as indicated in the Materials and Methods. One microliter of cDNA mixture was used in each reaction in lanes 1 to 18; 1 μl (2 ng) of DNA was used in control reactions (lanes 19 to 23). Lanes: M, size markers; 1, WCS358 (primer pair SAL01-SAL02); 2, WCS358 (Fe^{3+}) (SAL01-SAL02); 3, WCS358 (KM01/KM02); 4, WCS358 (Fe^{3+}) (KM01-KM02); 5, WCS374 (SAL01-SAL02); 6, WCS374 (Fe^{3+}) (SAL01-SAL02); 7, WCS374 (KM01-KM02); 8, WCS374 (Fe^{3+}) (KM01-KM02); 9, 374-08 (SAL01-SAL02); 10, 374-08 (Fe^{3+}) (SAL01-SAL02); 11, 374-08 (HDC01-SAL02); 12, 374-08 (Fe^{3+}) (HDC01-SAL02); 13, 374-08 (DHB01-DHB02); 14, 374-08 (Fe^{3+}) (DHB01-DHB02); 15, 374-08 (KM01-KM02); 16, 374-08 (Fe^{3+}) (KM01-KM02); 17, WCS374 (DHB01-DHB02); 18, WCS374 (Fe^{3+}) (DHB01-DHB02); 19, 374-08 DNA (SAL01-SAL02); 20, 374-08 DNA (HDC01-SAL02); 21, 374-08 DNA (DHB01-DHB02); 22, 374-08 DNA (KM01-KM02); 23, WCS374 DNA (KM01-KM02); 24, WCS374 DNA (2 μg) treated with RNase-free DNase (SAL01-SAL02); 25, 374-08 DNA (2 μg) treated with RNase-free DNase (KM01-KM02). (C) Dilution series of cDNA samples (1 μl) used in PCR experiments to estimate repression level upon Fe^{3+} addition. Primers used were SAL01-SAL02 for *pmsB* expression (214-bp PCR band) and KM01-KM02 for *neo* expression (405-bp PCR band). All lanes correspond to cDNA obtained from total RNA of 374-08. Odd-numbered lanes correspond to minimal-iron conditions; even-numbered lanes to 100 μM Fe^{3+}. Lanes 1 to 4, 1 μl of the cDNA original mixture; lanes 5 to 8, 5-fold-diluted samples; lanes 9 to 12, 25-fold-diluted samples; lanes 13 to 16, 125-fold-diluted samples; lanes 17 to 20, 625-fold-diluted samples; lanes 21 to 24, 3,125-fold-diluted samples.

tions (Fig. 3C). These results demonstrate that the promoter region detected by DNA analysis is functional and that the *pmsCEAB* genes may constitute an operon. However, further analysis will be necessary to confirm this organization. Finally, *pms* gene expression is iron regulated, suggesting that the iron-regulatory elements detected in the promoter region are functional as well.

DISCUSSION

Several strains of *Pseudomonas* spp. have been reported to produce more than one type of siderophore under iron-limiting conditions (2, 11, 43, 64). For the PGPR strain *P. fluorescens* WCS374, production of an additional siderophore, besides pseudobactin and SA, was suggested (33). In this work, we show that the additional siderophore in strain WCS374 is pseudomonine, an isoxazolidone previously isolated in culture supernatants of iron-deficient cultures of a *P. fluorescens* strain isolated on spoiled Nile perch from Lake Victoria (Africa) (3).

Two lines of evidence suggest that SA production and pseudomonine synthesis are related. One mutant that we studied (374-05) is impaired in both SA and pseudomonine production, and a recombinant cosmid from the WCS374 gene library carries the genetic information for both traits. Additionally, pseudomonine has been identified as an SA-based siderophore (reference 3 and this work). SA and pseudomonine biosynthe-

sis genes are closely linked and present in the recombinant clone pMB374-07. This plasmid induced both siderophore activity and SA production in *P. putida* WCS358 Psb-deficient strain JM218. pMB374-07 derivative subclones were unable to drive pseudomonine synthesis, suggesting that most of the cloned insert is involved in this trait. However, only 5 kb from pMB374-07 were required to induce SA production in JM218 (plasmids p07E3 and p07E3R) and in *E. coli* cells (plasmids pE3 and pE3R).

Double mutants impaired in the production of both pseudobactin and pseudomonine still showed some siderophore activity in CAS medium. Although additional iron uptake systems could still be functional, the possibility that mutant 374-05 is leaky and able to release small quantities of pseudomonine to the medium cannot be ruled out. As a matter of fact, HPLC analysis of the culture supernatant of mutant 374-05.8 revealed a very small peak at the position of pseudomonine (data not shown), indicating that the mutant indeed is leaky. Preliminary experiments have shown that the Tn*5* insertion in mutant 374-05 is located elsewhere in the WCS374 genome and that this mutant is likely affected in pseudomonine transport machinery (J. Mercado-Blanco, unpublished data).

Serino et al. (56) proposed that SA synthesis in *P. aeruginosa* proceeds from chorismate via isochorismate. The two potential SA biosynthesis genes of strain WCS374, *pmsC* and *pmsB*, showed moderate to high similarity to the SA biosynthetic genes *pchB* and *pchA* of *P. aeruginosa* (56); PchA would act as an ICS, and PchB would act as an isochorismate-pyruvate lyase. Based on sequence similarities, *pmsC* and *pmsB* may function similarly in *P. fluorescens* WCS374. However, the genetic organization is different. In *P. aeruginosa*, *pchB* and *pchA* are the distal genes of the *pchDCBA* operon involved in SA and pyochelin biosynthesis (57). In *P. fluorescens* WCS374, two genes are interspersed between the proposed SA biosynthetic genes (*pmsC* and *pmsB*): a putative *entE* homolog (*pmsE*) and a putative hdc gene (*pmsA*). It is unlikely that there is any role in SA synthesis for these latter genes, especially *pmsA* with a totally unrelated activity. We speculated that this genetic arrangement is part of the biosynthetic machinery of pseudomonine. *pmsC* and *pmsB* would contribute to synthesis of the SA moiety present in the pseudomonine structure. The presence of an *hdc* gene (*pmsA*) supports the conclusion that histamine, which is present in the structure of pseudomonine, is a precursor in the synthesis of this siderophore. Anguibactin in *V. anguillarum* (62) and acinetobactin in *A. baumannii* (65) are siderophores that also contain this biogenic amine. Acinetobactin and pseudomonine possess an oxazoline ring instead of a thiazoline ring which is present in anguibactin. Finally, PmsE has striking similarities to proteins involved in the biosynthesis of siderophores such as enterobactin (EntE), pyochelin (PchD), vibriobactin (VibE), and yersiniabactin (YbtE). The EntE protein mediates the activation of a catechol (2,3-DHB) in one of the steps in enterobactin synthesis. As proposed by Serino et al. (57) and previously reported for EntE of *E. coli* (35), PmsE might act in the same way as EntE, activating the carboxylate group of SA.

In vivo SA biosynthesis was achieved in heterologous backgrounds such as in *P. putida* and *E. coli* cells (Table 2). Similarly, *pms* genes were expressed under the control of their own promoter in *E. coli* (Table 2). Only when ORFD (*pmsB*) was not present was SA production impaired. When *pmsB* was provided alone (plasmid pJMSa1-10), SA was still detectable in M9 medium supernatant (Table 2). Thus, *pmsB* has been shown to be essential for SA synthesis in *E. coli*. This observation indicates that PmsB can use endogenous substrates provided by *E. coli* cells. However, upstream genes appear to provide additional substrates to produce high SA levels (plasmids pE3 and pE3R [Table 2]). Serino et al. (56) concluded that PchB in *P. aeruginosa* seems to be involved in the conversion of isochorismate to SA, but it is unable to synthesize SA directly from chorismate. The fact that SA was detected in DH5α harboring deletion plasmids affecting *pmsC* indicates that this gene is not essential for SA biosynthesis in *E. coli* but is important to reach the SA levels produced by pE3R. An explanation may be that indigenous ICS activity complements the absence of PmsC in deletion clones. Alternatively, substrates provided by *E. coli* can be used, with less specificity, by PmsB. In contrast, SA was not detected in JM218 culture supernatants when *pmsB* was provided alone (pLASa1-10). PmsB has a certain degree of homology with the N-terminal domain of different chorismate mutases. An interesting possibility, which require further experimental support, is that the putative PmsB can use other substrates, including chorismate. In this sense, moderate homology (29% identity and 59% similarity) was found with the 129-amino-acid-residue protein PapB from *Streptomyces pristinaespiralis*, a protein identified as a mutase involved in the biosynthesis of 4-methylamino-L-phenylalanine (accession number P72541). It is also interesting that PmsB showed homology with an unknown ORF in *V. vulnificus*. This bacterium synthesizes vulnibactin, a siderophore which contains two residues of SA (46). These two residues are involved in the formation of oxazoline rings with L-threonine, the same arrangement as encountered in pseudomonine. Thus, PmsB, PchB, and the latter ORF may constitute a family of proteins involved in synthesis of the SA moiety in this type of siderophore.

Results of homology analysis presented in this work, along with the results of gene expression by RT-PCR as well as Fe-mediated SA synthesis repression studies performed earlier by our group (33), show that (i) the promoter region detected upstream of *pmsC* is functional, (ii) expression of the *pms* genes is iron regulated, and (iii) the *pmsCEAB* transcript is polycistronic. However, the existence of additional promoters in the *pms* region cannot be completely ruled out. Differences in efficiency in primer binding can be considered, although no obvious differences were observed when DNA templates were used in PCR control experiments (Fig. 3B).

The specific contributions of pseudobactin, pseudomonine, and SA in iron uptake in strain WCS374 are not known. On the other hand, it has been demonstrated that pseudobactin and SA induce resistance in radishes against *Fusarium* wilt (33). These authors reported that a pseudobactin mutant was still able to induce resistance at low iron availability, hypothesizing that SA or a different siderophore, which now has been confirmed to be pseudomonine, was responsible for disease suppression. The possible role of pseudomonine in plant disease suppression and ISR will be further investigated.

ACKNOWLEDGMENTS

We are very grateful to Carsten Christophersen, Marine Chemistry Section, Chemical Institute, University of Copenhagen, Copenhagen, Denmark, for sharing unpublished FAB and EI mass spectra recorded from his group's original pseudomonine sample. We thank Truus Hooijmakers (Hubrecht Laboratorium, Utrecht, The Netherlands) for DNA sequencing. We are also grateful to Bert Simons for interesting discussions and helpful suggestions regarding RT-PCR.

J. M.-B. is indebted to Spanish Consejo Superior de Investigaciones Científicas and the European Union (ERBCHBICT941786) for postdoctoral fellowships.

REFERENCES

1. **Altschul, S. F., W. Gish, W. Miller, E. W. Myers, and D. J. Lipman.** 1990. Basic local alignment search tool. J. Mol. Biol. **215:**403–410.
2. **Ankenbauer, R. G., and C. D. Cox.** 1988. Isolation and characterization of *Pseudomonas aeruginosa* mutants requiring salicylic acid for pyochelin biosynthesis. J. Bacteriol. **170:**5364–5367.
3. **Anthoni, U., C. Christophersen, P. H. Nielsen, L. Gram, and B. O. Petersen.** 1995. Pseudomonine, an isoxazolidone with siderophoric activity from *Pseudomonas fluorescens* AH2 isolated from Lake Victorian Nile perch. J. Nat. Prod. **58:**1786–1789.
4. **Arnow, L. E.** 1937. Colorimetric determination of the components of 3,4-dihydroxyphenylalanine-tyrosine mixtures. J. Biol. Chem. **118:**531–537.
5. **Bakker, P. A. H. M., J. G. Lamers, A. W. Bakker, J. D. Marugg, P. J. Weisbeek, and B. Schippers.** 1986. The role of siderophores in potato tuber yield increase by *Pseudomonas putida* in a short rotation of potato. Neth. J. Plant Pathol. **92:**249–256.
6. **Barghouthi, S., S. M. Payne, J. E. L. Arceneaux, and B. R. Byers.** 1991. Cloning, mutagenesis, and nucleotide sequence of a siderophore biosynthetic gene (*amoA*) from *Aeromonas hydrophila*. J. Bacteriol. **173:**5121–5128.
7. **Beck, E., G. Ludwig, E. A. Auerswald, B. Reiss, and H. Schaller.** 1982. Nucleotide sequence and exact localization of the neomycin phosphotransferase gene from transposon Tn*5*. Gene **19:**327–336.
8. **Biek, D., and J. R. Roth.** 1980. Regulation of Tn*5* transposition in *Salmonella typhimurium*. Proc. Natl. Acad. Sci. USA **77:**6047–6051.
9. **Birnboim, H. C., and J. Doly.** 1979. A rapid alkaline extraction procedure for screening recombinant plasmid DNA. Nucleic Acids Res. **7:**1513–1523.
10. **Boyer, H. W., and D. Roulland-Dussoix.** 1969. A complementation analysis of restriction and modification in *Escherichia coli*. J. Mol. Biol. **41:**459–472.
11. **Buysens, S., K. Heungens, J. Poppe, and M. Höfte.** 1996. Involvement of pyochelin and pyoverdine in suppression of *Pythium*-induced damping-off of tomato by *Pseudomonas aeruginosa* 7NSK2. Appl. Environ. Microbiol. **62:**865–871.
12. **Carmi, R., S. Varmeli, E. Levy, and F. J. Gough.** 1994. (+)-(S)-dihydroaeruginoic acid, an inhibitor of *Septoria tritici* and other phytopathogenic fungi and bacteria, produced by *Pseudomonas fluorescens*. J. Nat. Prod. **57:**1200–1205.
13. **Cox, C. D., and R. Graham.** 1978. Isolation of an iron-binding compound from *Pseudomonas aeruginosa*. J. Bacteriol. **137:**357–364.
14. **Cox, C. D., K. L. Rinehart, M. L. Moore, and J. C. Cook.** 1981. Pyochelin: novel structure of an iron-chelating growth promoter for *Pseudomonas aeruginosa*. Proc. Natl. Acad. Sci. USA **78:**4256–4260.
15. **Csáky, T. Z.** 1948. On the estimation of bound hydroxylamine in biological materials. Acta Chem. Scand. **2:**450–454.
16. **de Lorenzo, V., S. Wee, M. Herrero, and J. B. Neilands.** 1987. Operator sequences of the aerobactin operon of plasmid ColV-K30 binding the ferric uptake regulation (*fur*) repressor. J. Bacteriol. **169:**2624–2630.
17. **de Meyer, G., C. Capieau, K. Audenaert, A. Buchala, J.-P. Metraux, and M. Höfte.** 1999. Nanogram amounts of salicylic acid produced by the rhizobacterium *Pseudomonas aeruginosa* 7NSK2 activate the systemic acquired resistance pathway in bean. Mol. Plant-Microbe Interact. **12:**450–458.
18. **de Meyer, G., and M. Höfte.** 1997. Salicylic acid produced by the rhizobacterium *Pseudomonas aeruginosa* 7NSK2 induces resistance to leaf infection by *Botrytis cinerea* on bean. Phytopathology **87:**588–593.
19. **Elkins, M. F., and C. F. Earhart.** 1988. An *Escherichia coli* enterobactin cluster gene with sequence homology to *trpE* and *pabB*. FEMS Microbiol. Lett. **56:**35–40.
20. **Figurski, D. H., and D. R. Helinski.** 1979. Replication of an origin-containing derivative of plasmid RK2 dependent on a plasmid function provided in *trans*. Proc. Natl. Acad. Sci. USA **76:**1648–1652.
21. **Friedman, A. M., S. R. Long, S. E. Brown, W. J. Buikema, and F. Ausubel.** 1982. Construction of a broad host range cosmid cloning vector ant its use in the genetic analysis of *Rhizobium meliloti*. Gene **18:**289–296.
22. **Geels, F. P., and B. Schippers.** 1983. Selection of antagonistic fluorescent *Pseudomonas* spp. and their root colonization and persistence following treatment of seed potatoes. J. Phytopathol. **108:**193–206.
23. **Geornaras, I., G. A. Dykes, and A. von Holy.** 1995. Biogenic amine formation by poultry-associated spoilage and pathogenic bacteria. Lett. Appl. Microbiol. **21:**164–166.
24. **Gray, J. V., B. Golinelli-Pimpaneau, and J. R. Knowles.** 1990. Monofunctional chorismate mutase from *Bacillus subtilis*: purification of the protein, molecular cloning of the gene, and overexpression of the gene product in *Escherichia coli*. Biochemistry **29:**376–383.
25. **Hayashi, H., S. Tanase, and E. Snell.** 1986. Pyridoxal 5′-phosphate-dependent histidine decarboxylase. J. Biol. Chem. **261:**11030–11009.
26. **Höfte, M.** 1993. Classes of microbial siderophores, p. 3–26. *In* L. L. Barton and B. C. Hemming (ed.), Iron chelation in plants and soil microorganisms. Academic Press, San Diego, Calif.
27. **Hudson, A. T., and R. Bentley.** 1970. Utilization of shikimic acid for the formation of mycobactin S and salicylic acid by *Mycobacterium smegmatis*. Biochemistry **9:**3984–3987.
28. **Hynes, M. F., J. Quandt, M. P. O'Connell, and A. Pühler.** 1989. Direct selection for curing and deletion of *Rhizobium* plasmids using transposons carrying the *Bacillus subtilis sacB* gene. Gene **78:**111–120.
29. **Jalal, M., D. Hossain, J. van der Helm, J. Sanders-Loehr, L. A. Actis, and J. H. Crosa.** 1989. Structure of anguibactin, a unique plasmid-related bacterial siderophore from the fish pathogen *Vibrio anguillarum*. J. Am. Chem. Soc. **111:**292–296.
30. **Kamath, A. V., G. L. Vaaler, and E. Snell.** 1991. Pyridoxal phosphate-dependent histidine decarboxylase. J. Biol. Chem. **266:**9432–9437.
31. **Keller-Schierlein, W., L. Hagmann, H. Zähner, and W. Huhn.** 1988. Maduraferrin, a novel siderophore from *Acinomadura madurae*. Helv. Chim. Acta **71:**1528–1534.
32. **King, E. O., M. K. Ward, and D. E. Raney.** 1954. Two simple media for demonstration of pyocyanin and fluorescin. J. Lab. Clin. Med. **44:**301–307.
33. **Leeman, M., F. M. den Ouden, J. A. van Pelt, F. P. M. Dirkx, H. Steijl, P. A. H. M. Bakker, and B. Schippers.** 1996. Iron availability affects induction of systemic resistance to Fusarium wilt of radish by *Pseudomonas fluorescens*. Phytopathology **86:**149–155.
34. **Lemanceau, P., P. A. H. M. Bakker, W. J. De Kogel, C. Alabouvette, and B. Schippers.** 1992. Effect of pseudobactin 358 production by *Pseudomonas putida* WCS358 on suppression of *Fusarium* wilt of carnations by nonpathogenic *Fusarium oxysporum* Fo47. Appl. Environ. Microbiol. **58:**2978–2982.
35. **Liu, J., K. Duncan, and C. T. Walsh.** 1989. Nucleotide sequence of a cluster of *Escherichia coli* enterobactin biosynthesis genes: identification of *entA* and purification of its product 2,3-dihydro-2,3-dihydroxybenzoate dehydrogenase. J. Bacteriol. **171:**791–798.
36. **Loper, J. E., and J. S. Buyer.** 1991. Siderophores in microbial interactions on plant surfaces. Mol. Plant-Microbe Interact. **4:**5–13.
37. **Loper, J. E., C. A. Ishimaru, S. R. Carnegie, and A. Vanavivhit.** 1993. Cloning and characterization of the aerobactin biosynthesis genes of the biological control agent *Enterobacter cloacae*. Appl. Environ. Microbiol. **59:**4189–4197.
38. **Marshall, B. J., and C. Ratledge.** 1971. Conversion of chorismic acid and isochorismic acid to salicylic-acid by cell-free extracts of *Mycobacterium smegmatis*. Biochim. Biophys. Acta **230:**643–645.
39. **Marugg, J. D., M. van Spanje, W. P. M. Hoekstra, B. Schippers, and P. J. Weisbeek.** 1985. Isolation and analysis of genes involved in siderophore biosynthesis in plant-growth-stimulating *Pseudomonas putida* WCS358. J. Bacteriol. **164:**563–570.
40. **Maurhofer, M., C. Hase, P. Meuwly, J.-P. Métraux, and G. Défago.** 1994. Induction of systemic resistance of tobacco to tobacco necrosis virus by the root-colonizing *Pseudomonas fluorescens* strain CHAO: influence of the *gacA* gene and the pyoverdine production. Phytopathology **84:**139–146.
41. **Maurhofer, M., C. Reimann, P. Schimidli-Sachrer, S. Heeb, D. Haas, and G. Défago.** 1998. Salicylic acid biosynthesis genes expressed in *Pseudomonas fluorescens* strain P3 improve the induction of systemic resistance in tobacco against tobacco necrosis virus. Phytopathology **88:**678–684.
42. **Meyer, J.-M., and M. A. Abdallah.** 1978. The fluorescent pigment of *Pseudomonas fluorescens*: biosynthesis, purification and physicochemical properties. J. Gen. Microbiol. **107:**319–328.
43. **Meyer, J.-M., P. Azelvandre, and C. Georges.** 1992. Iron metabolism in *Pseudomonas*: salicylic acid, a siderophore of *Pseudomonas fluorescens* CHAO. Biofactors **4:**23–27.
44. **Miller, J. H.** 1972. Experiments in molecular genetics. Cold Spring Harbor Laboratory, Cold Spring Harbor, N.Y.
45. **Neilands, J. B., K. Konopka, B. Schwyn, M. Coy, R. T. Francis, B. H. Paw, and A. Bagg.** 1987. Comparative biochemistry of microbial iron assimilation, p. 3–33. *In* G. Winkelmann, D. van der Helm, and J. B. Neilands (ed.), Iron transport in microbes, plants and animals. Verlagsgesellschaft mbH, Weinheim, Germany.
46. **Okujo, N., M. Saito, S. Yamamoto, T. Yoshida, S. Miyoshi, and S. Shinoda.** 1994. Structure of vulnibactin, a new polyamine-containing siderophore from *Vibrio vulnificus*. BioMetals **7:**109–116.
47. **Person, T., and J. B. Neilands.** 1979. Revised structure of a catecholamide spermidine siderophore from *Paracoccus denitrificans*. Tetrahedron Lett. **50:**485–4808.
48. **Rajagopalan, J. S., K. M. Taylor, and E. Jaffe.** 1993. ^{13}C NMR studies of the enzyme-product complex of *Bacillus subtilis* chorismate mutase. Biochemistry **32:**3965–3972.
49. **Ratledge, C.** 1964. Relationship between the products of aromatic biosyn-

thesis in *Mycobacterium smegmatis* and *Aerobacter aerogenes*. Nature **203:** 428–429.
50. **Ratledge, C., and M. J. Hall.** 1972. Isolation and properties of auxotrophic mutants of *Mycobacterium smegmatis* requiring either salicylic acid or mycobactin. J. Gen. Microbiol. **72:**143–150.
51. **Ratledge, C., and F. G. Winder.** 1962. The accumulation of salicylic acid in mycobacteria during growth on iron-deficient medium. Biochemistry **84:**501–506.
52. **Rioux, C., D. C. Jordan, and J. B. M. Rattray.** 1983. Colorimetric determination of catechol siderophores in microbial cultures. Anal. Biochem. **133:** 163–169.
53. **Sambrook, J., E. F. Fritsch, and T. Maniatis.** 1989. Molecular cloning: a laboratory manual, 2nd ed. Cold Spring Harbor Laboratory, Cold Spring Harbor, N.Y.
54. **Saxena, B., M. Mayuranki, and V. V. Modi.** 1986. Isolation and characterization of siderophores from *Azospirillum lipoferum* D-2. J. Gen. Microbiol. **132:**2219–2224.
55. **Schwyn, B., and J. B. Neilands.** 1987. Universal chemical assay for the detection and determination of siderophores. Anal. Biochem. **160:**47–56.
56. **Serino, L., C. Reimmann, H. Baur, M. Beyeler, P. Visca, and D. Haas.** 1995. Structural genes for salicylate biosynthesis from chorismate in *Pseudomonas aeruginosa*. Mol. Gen. Genet. **249:**217–228.
57. **Serino, L., C. Reimmann, P. Visca, M. Beyeler, V. della Chiesa, and D. Haas.** 1997. Biosynthesis of pyochelin and dihydroaeruginoic acid requires the iron-regulated *pchDCBA* operon in *Pseudomonas aeruginosa*. J. Bacteriol. **179:**248–257.
58. **Shine, J., and L. Dalgarno.** 1974. The 3′ terminal sequence of *Escherichia coli* 16S RNA: complementarity to nonsense triplets and ribosome binding sites. Proc. Natl. Acad. Sci. USA **71:**1342–1346.
59. **Simon, R., U. Priefer, and A. Pühler.** 1983. A broad host range mobilization system for *in vivo* genetic engineering: transposon mutagenesis in gram-negative bacteria. Bio/Technology **1:**784–791.
60. **Snow, G. A.** 1965. Isolation and structure of mycobactin T, a growth factor from *Mycobacterium tuberculosis*. Biochem. J. **97:**166–175.
61. **Sokol, P. A., C. J. Lewis, and J. J. Dennis.** 1992. Isolation of a novel siderophore from *Pseudomonas cepacia*. J. Med. Microbiol. **36:**184–189.
62. **Tolmasky, M. E., L. A. Actis, and J. H. Crosa.** 1995. A histidine decarboxylase gene encoded by the *Vibrio anguillarum* plasmid pJM1 is essential for virulence: histamine is a precursor in the biosynthesis of anguibactin. Mol. Microbiol. **15:**87–95.
63. **van Loon, L. C., P. A. H. M. Bakker, and C. M. J. Pieterse.** 1998. Systemic resistance induced by rhizosphere bacteria. Annu. Rev. Phytopathol. **36:**453–483.
64. **Visca, P., A. Ciervo, V. Sanfilippo, and N. Orsi.** 1993. Iron-regulated salicylate synthesis by *Pseudomonas* spp. J. Gen. Microbiol. **139:**1995–2001.
65. **Yamamoto, S., N. Okujo, and Y. Sakakibara.** 1994. Isolation and structure elucidation of acinetobactin, a novel siderophore from *Acinetobacter baumannii*. Arch. Microbiol. **162:**249–254.